AMERICAN SOCIETY FOR MICROBIOLOGY | Journal of Virology®

CELLULAR RESPONSE TO INFECTION

Serial Passaging of the Human Rotavirus CDC-9 Strain in Cell Culture Leads to Attenuation: Characterization from *In Vitro* and *In Vivo* Studies

Theresa Kathrina Resch,[a] Yuhuan Wang,[b] Sungsil Moon,[b] Baoming Jiang[b]

[a]Cherokee Nation Assurance, for Division of Viral Diseases, Centers for Disease Control and Prevention, Atlanta, Georgia, USA
[b]Division of Viral Diseases, Centers for Disease Control and Prevention, Atlanta, Georgia, USA

ABSTRACT Live oral rotavirus vaccines have been developed by serial passaging in cell culture and found to be safe in infants. However, mechanisms for the adaptation and attenuation of rotavirus vaccines are not fully understood. We prepared a human rotavirus vaccine strain, CDC-9 (G1P[8]), which when grown in MA104 cells to passage 11 or 12 (P11/P12) had no nucleotide or amino acid sequence changes from the original virus in stool. Upon adaptation and passages in Vero cells, the strain underwent five amino acid changes at P28 and one additional change at P44/P45 in the VP4 gene. We performed virologic, immunological, and pathogenic characterization of wild-type CDC-9 virus at P11/P12 and its two mutants at P28 or P44/P45 using *in vitro* and *in vivo* model systems. We found that mutants CDC-9 P28 and P44 induced upregulated expression of immunomodulatory cytokines. On the other hand, the two mutant viruses induced lower STAT1 phosphorylation and grew to 2-log-higher titers than wild-type virus in human Caco-2 cells and simian Vero cells. In neonatal rats, CDC-9 P45 showed reduced rotavirus shedding in fecal specimens and did not induce diarrhea compared to wild-type virus and modulated cytokine responses comparably to Rotarix infection. These findings indicate that mutant CDC-9 is attenuated and safe. Our study is the first to provide insight into the possible mechanisms of human rotavirus adaptation and attenuation and supports ongoing efforts to develop CDC-9 as a new generation of rotavirus vaccine for live oral or parenteral administration.

IMPORTANCE Mechanisms for *in vitro* adaptation and *in vivo* attenuation of human rotavirus vaccines are not known. The present study is the first to comprehensively compare the *in vitro* growth characteristics, virulence, and host response of a wild-type and an attenuated human rotavirus strain, CDC-9, in Caco-2 cells and neonatal rats. Our study identifies critical sequence changes in the genome that render human rotavirus adapted to growth to high levels in Vero cells and attenuated and safe in neonatal rats; thus, the study supports clinical development of CDC-9 for oral or parenteral vaccination in children.

KEYWORDS rotavirus, vaccine, virus attenuation, oral vaccines, virus adaptation

Serial passaging of viruses in cell culture for various periods of time has commonly been used to develop vaccines against diseases like polio, measles, mumps, rubella, and varicella (1–6). These serial passages in cell culture have led to limited but defined sequence changes in viral genomes, resulting in the adaptation and selection of virus mutants that are best suited to growth in specific cell lines. These virus mutants have modifications or loss of virulence factors that usually allow them to infect and spread within a human host (7). Tissue culture-adapted viruses are able to replicate more

Citation Resch TK, Wang Y, Moon S, Jiang B. 2020. Serial passaging of the human rotavirus CDC-9 strain in cell culture leads to attenuation: characterization from *in vitro* and *in vivo* studies. J Virol 94:e00889-20. https://doi.org/10.1128/JVI.00889-20.

Editor Susana López, Instituto de Biotecnologia/UNAM

Address correspondence to Baoming Jiang, bxj4@cdc.gov.

Received 7 May 2020
Accepted 12 May 2020
Accepted manuscript posted online 27 May 2020
Published 16 July 2020

efficiently in cells than wild-type strains (8), an important requirement for scaled-up vaccine production.

Similarly, currently licensed human oral rotavirus (RV) vaccines, like Rotarix, Rotavac and Rotavin, have been developed by serial passaging in cell culture and are found attenuated in humans (9–11). For example, the G1P[8] human RV strain 89-12 (ancestor of Rotarix) was passaged 33 times in primary African green monkey (AGMK) cells (12), and upon further limiting dilutions and passages in Vero cells, the strain was found attenuated in adults and seropositive children (11). Infants who were inoculated with strain 89-12 shed significantly less RV antigen than those with natural RV infection and did not develop diarrhea (12). However, no comprehensive studies have been carried out to investigate the mechanisms of attenuation and the immune responses generated by wild-type and attenuated RV.

The RV genome consists of 11 segments of double-stranded RNA encoding 6 structural proteins (VP1 to VP4, VP6, and VP7) and 5 nonstructural proteins (NSP1 to NSP5) (13). Of the 11 viral proteins, VP4 and NSP1 have shown to be determining factors for virulence and host restriction of RV in newborn mice (14–16). In addition, VP3, VP7, and NSP4 were found to play an important role in the virulence of RV infection in gnotobiotic piglets (17). RV infection stimulates the production of type I and II interferons (IFNs) in children (18, 19). On the other hand, RV NSP1 is known to antagonize type I IFN production by proteasomal degradation of IFN-regulatory factors (IRFs), which are essential transcription factors for innate immunity (20, 21), or by inhibition of type I IFN-mediated signal transducer and activator of transcription 1 (STAT1) activation and nuclear translocation (22, 23).

We previously reported the isolation and characterization of the human candidate RV vaccine CDC-9 and found that the strain was able to grow in permissive African green monkey kidney cells (MA104) without any sequence changes (24). However, we observed that the strain underwent limited nucleotide and amino acid changes in several genes during adaptation and 28 passages (P28) in Vero cells. CDC-9 underwent few changes in the genome upon further passages (P44/P45) in Vero cells. In this study, we compared the *in vitro* growth characteristics, virulence, and host responses of CDC-9 grown in MA104 cells (P11 or P12), designated "wild type" due to the lack of sequence changes in the first 11 or 12 passages, and two CDC-9 mutants from intermediate (P28) and late (P44 or P45) passages in Vero cells, in a human intestinal epithelial carcinoma cell line (Caco-2) and neonatal rats. We showed that CDC-9 mutants were well adapted and grew to titers almost 2 logs higher than their wild-type counterpart in Caco-2 cells. We further showed that mutant CDC-9 P45 was attenuated and safe and induced innate immune responses that were comparable to those induced by Rotarix infection in neonatal rats.

RESULTS

We analyzed nucleotide and amino acid sequences of CDC-9 in stool, MA104 cells (P11 or P12), and Vero cells (P28, P44, and P45) by Sanger or next-generation sequencing methods (Table 1). No differences in the nucleotide sequence of CDC-9 virus from original stool relative to P11/P12 in MA104 cells were observed. Thus, CDC-9 P11/P12 was considered a wild-type virus. On the other hand, we observed 5 amino acid changes in the VP4 gene and a single amino acid change each in the VP6, NSP1, and NSP5 genes when the virus was adapted and propagated to P28 in Vero cells. One additional amino acid change in the VP1 gene and the VP4 gene and a 10-amino acid deletion in VP2 gene were observed when the virus was further propagated to P44/P45 in Vero cells.

To determine whether sequence changes during serial passages in Vero cells led to differences in viral growth, we compared the infectivity of CDC-9 strains between wild-type P11 virus in MA104 cells and mutant viruses from intermediate-passage (P28) and late-passage (P44) virus in Vero cells and Caco-2 cells (Fig. 1). We found that both CDC-9 P28 and P44 grew to titers of 10^6 to 10^7 focus-forming units (FFU)/ml, which was approximately 2 logs higher than wild-type CDC-9 P11 ($P < 0.01$). These data indicate

TABLE 1 Nucleotide and amino acid sequence changes for CDC-9 P11/12, CDC-9 P28, and CDC-9 P44/45[a]

Gene segment	No. of CDC-9 P11/12 NT changes	CDC-9 P28				CDC-9 P44/45			
		No. of NT changes	NT position(s)	No. of aa changes	aa position(s)	No. of NT changes	NT position(s)	No. of aa changes	aa position(s)
VP1	None	None				1	3146	1	1043
VP2	None	None				30	100–130	10	27–36
VP3	None	None				2	391, 1639	None	
VP4	None	6	161, 1001, 1101, 1162, 1171, 2025	5	51, 331, 364, 385, 388	8	161, 1001, 1101, 1162, 1171, 1504, 1785, 2025	6	51, 331, 364, 385, 388, 498
VP6	None	1	325	1	101	1	325	1	101
VP7	None	1	678	None		2	678, 1052	None	
NSP1	None	1	396	1	132	1	396	1	132
NSP2	None	None				None			
NSP3	None	None				None			
NSP4	None	None				None			
NSP5	None	1	155	1	45	1	155	1	45

[a]NT, nucleotide; aa, amino acid.

that a small number of amino acid changes in several genes of CDC-9 P28 and P44 might have contributed to their enhanced growth in Caco-2 cells. Similarly, mutant CDC-9 showed enhanced growth in Vero cells relative to the wild-type virus.

We assessed host responses to wild-type and mutant viruses by examining the expression of transcription factor STAT1 in Caco-2 cells (Fig. 2A). CDC-9 P11 induced significantly elevated levels of STAT1 phosphorylation (p-STAT1) compared to mock infection at 6 and 24 h postinfection (hpi). Levels of STAT1 phosphorylation after CDC-9 P11 infection were similar to those from rhesus monkey RV (RRV) infections (6 hpi, $P = 0.1$; 24 hpi, $P = 0.061$). In contrast, CDC-9 P28 induced a smaller increase at 24 hpi and P44 induced no elevation in STAT1 phosphorylation at 6 and 24 hpi compared to mock infections. In controls, the intracellular pan-STAT1 levels were unchanged from virus infection and comparable among all groups throughout the experiment. Similar patterns of STAT1 expression were also observed in Caco-2 cells by Western blot analysis (Fig. 2B). STAT1 phosphorylation increased 24 hpi with CDC-9 P11; this increase was not seen in cells infected with CDC-9 P28 and CDC-9 P44 at 6 and 24 hpi. In control, RRV induced increased STAT1 phosphorylation at 6 and 24 hpi. We did not observe any differences in phosphorylation for any other members of the STAT family, including STAT2, STAT3, STAT5, and STAT6.

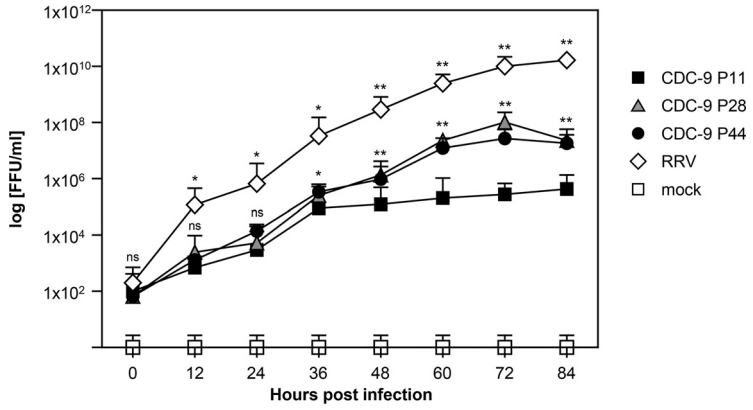

FIG 1 Growth curves of wild-type and mutant CDC-9 in human intestinal epithelial cells (Caco-2). Caco-2 cells were infected with CDC-9 P11, P28, or P44 or RRV at an MOI of 0.1 or mock treated in the same manner. At the indicated time points, infected cultures were collected, and titration was performed in MA104 cells. The data are means and 3 standard errors from 3 independent experiments in triplicate ($n = 9$). Statistical analysis was performed to compare titers of CDC-9 P11 with those of CDC-9 P28, P44, or RRV by using a paired t test. Titers from CDC-9 P28- and P44-infected cultures were similar. ns, not significant ($P > 0.05$); *, $P \leq 0.05$; **, $P < 0.01$.

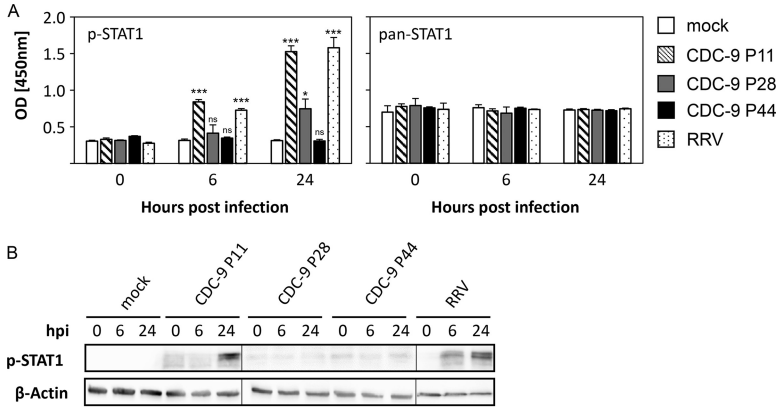

FIG 2 Wild-type CDC-9 induces increased STAT1 phosphorylation in Caco-2 cells. Caco-2 cells were infected with CDC-9 P11, P28, and P44 at an MOI of 0.2, harvested at 6 and 24 hpi, and analyzed for STAT1 phosphorylation (p-STAT1) by enzyme immunoassay (A) and Western blotting (B) as described in the text. The data in panel A for p-STAT1 are the averages and 3 standard errors from 2 experiments ($n = 9$) compared to pan-STAT1 expression. Images in panel B were generated from three different Western blots. Mock or RRV infections were used for controls. Statistical analysis was done to compare levels of STAT1 phosphorylation to that of CDC-9 infection and the mock infection control using a paired *t* test. ns, not significant ($P > 0.05$); *, $P \leq 0.05$; ***, $P < 0.001$.

We investigated whether mutant CDC-9 virus could change host responses by measuring expression of cytokines in the supernatants of Caco-2 cells infected with CDC-9 strains of different passages (Fig. 3A and B). Of the 16 cytokines tested, we detected significant elevation of interleukin 6 (IL-6), IL-9, IL-12p70, and monocyte-chemoattractant protein-1 (MCP-1) in supernatants of cells infected with CDC-9 P44 at 6 and 24 hpi, compared to those infected with CDC-9 P11 ($P = 0.008$) (Fig. 3A). Expression of those cytokines after infection with CDC-9 P28 showed an intermediate phenotype between those of CDC-9 P11 and CDC-9 P44. On the other hand, CDC-9 P28 and P44 induced significantly decreased expression of proinflammatory IL-1β, IL-8, and

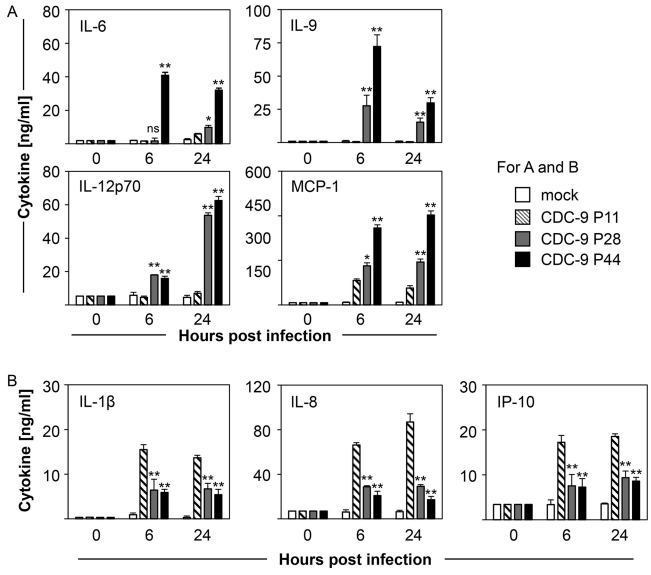

FIG 3 Mutant CDC-9 induces increased expression of immunomodulatory cytokines (A) and reduced expression of proinflammatory cytokines (B) in Caco-2 cells. Caco-2 cells were infected with CDC-9 P11, P28, and P44 at an MOI of 0.2 or mock treated, harvested at 6 and 24 hpi, and analyzed for cytokine expression by enzyme immunoassay as described in the text. The data are means and 3 standard errors from 3 independent experiments ($n = 9$). Statistical analysis was done to compare cytokine levels in CDC-9 or mock-infected cells using the Mann-Whitney test. ns, not significant ($P > 0.05$); *, $P \leq 0.05$; **, $P < 0.01$.

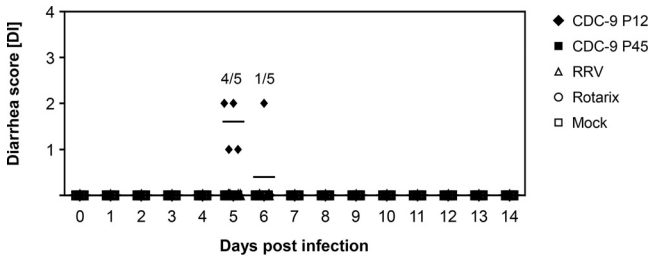

FIG 4 No induction of diarrhea from infection with mutant CDC-9 in neonatal rats. Five-day-old rat pups were inoculated with 1×10^6 FFU of the respective viruses or with clarified Vero cell culture supernatants in IMDM as a mock infection control. Diarrhea was scored daily for up to 14 days as described in the text. The data are individual diarrheal scores for 10 (days 0 to 4) and 5 (days 5 to 14) animals; the mean diarrheal score is indicated by the long dash.

IFN-γ-induced protein 10 (IP-10) compared to CDC-9 P11 infections at 6 and 24 hpi (P= 0.008) (Fig. 3B).

To determine whether mutant CDC-9 was attenuated, we orally inoculated 5-day-old neonatal rats with CDC-9 P12 (wild type) or CDC-9 P45, as well as Rotarix, RRV, or mock infection controls. We did not observe diarrhea in animals inoculated with mutant CDC-9 P45, Rotarix, or RRV or mock inoculated throughout the study period. However, 4 of 5 CDC-9 P12-inoculated animals on day 5 and 1 of 5 animals on day 6 had some loose stool with a diarrheal score of 1 or 2 (Fig. 4). We further assessed the infectivity and attenuation of CDC-9 P45 by analyzing RV shedding in rectal swabs of neonatal rats (Fig. 5). Animals infected with mutant CDC-9 P45 shed significantly less RV than those infected with wild-type CDC-9 P12 4 to 8 days postinfection (dpi). Overall, animals infected with the three human strains (wild-type CDC-9, mutant CDC-9, and Rotarix) had shedding profiles similar to but lower than those of animals infected with RRV, which shed the highest titers 2 to 8 dpi. No shedding was detected in mock-inoculated control animals.

To examine if mutant CDC-9 also modulated host response, we measured levels of cytokines and chemokines in sera of infected rats (Fig. 6). Animals infected with mutant CDC-9 P45 showed upregulation of immunomodulatory cytokines IL-6 ($P = 0.019$), IL-10 ($P = 0.020$), IL-18 ($P = 0.049$), and granulocyte-macrophage colony-stimulating factor (GM-CSF) ($P = 0.018$) on day 4 postinfection compared to wild-type CDC-9 P12 (Fig. 6A). On the other hand, the proinflammatory cytokines IFN-γ ($P = 0.040$) and IL-1α ($P = 0.006$) were significantly downregulated upon CDC-9 P45 infection compared to CDC-9

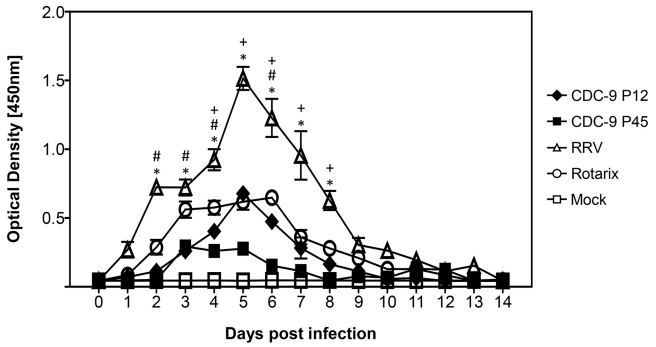

FIG 5 Reduced shedding in neonatal rats infected with mutant CDC-9 compared to wild-type virus. Five-day-old rat pups were inoculated with 1×10^6 FFU of the respective viruses or with clarified Vero cell culture supernatants in IMDM as a mock infection control. Rectal swabs were collected daily, and shedding was analyzed by Premier Rotaclone EIA for measuring the optical density. The data are means for 5 animals, with 3 standard errors. Differences in shedding among groups were analyzed using 2-way ANOVA with Bonferroni posttest comparison. A P value of $\leq$0.05 was considered significant for animals infected with CDC-9 P12 versus RRV (*), CDC-9 P12 versus Rotarix (#), and CDC-9 P12 versus CDC-9 P45 (+).

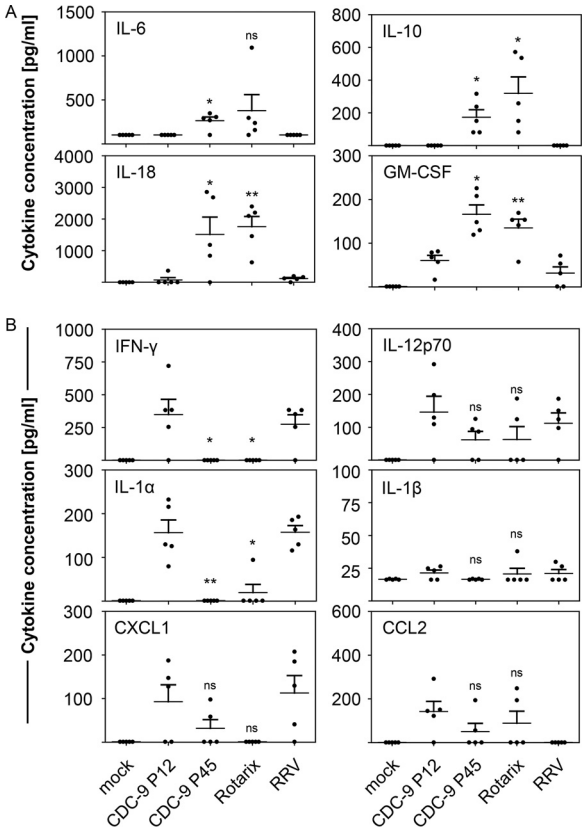

FIG 6 Mutant CDC-9 induces increased expression of immunomodulatory cytokines (A) and reduced expression of proinflammatory cytokines (B) in neonatal rats. Five-day-old rat pups were inoculated with 1×10^6 FFU of virus or clarified Vero cell culture supernatants in IMDM as a mock infection control. Serum specimens collected at 4 dpi were examined for cytokine concentration as described in the text. The data are means for 5 animals, with 3 standard errors. Statistical analysis was done to compare cytokine levels in CDC-9- and mock-infected cells using a paired *t* test. ns, not significant ($P > 0.05$); *, $P \leq 0.05$; **, $P < 0.01$.

P12 infection on day 4 postinfection (Fig. 6B). In addition, we observed a nonsignificant downregulation of the proinflammatory cytokines IL-12p70 ($P = 0.086$) and IL-1β ($P = 0.074$) and the chemokines CXCL1 ($P = 0.192$) and CCL2 ($P = 0.215$) after infection with CDC-9 P45 compared to CDC-9 P12 (Fig. 6B). Overall, cytokine and chemokine profiles resulting from infection with mutant CDC-9 P45 were similar to those from Rotarix infection, whereas similar profiles were seen with CDC-9 P12 and RRV infections. Mock-infected animals had no elevation in the cytokines examined. We did not observe any significant upregulation of cytokines or chemokines at 14 dpi in any of the groups.

Despite observed differences in infectivity and host response for wild-type and mutant CDC-9, all CDC-9-infected neonatal rats showed normal body weight gains comparable to Rotarix-infected and mock-treated animals (Fig. 7). We observed significantly less gain in body weight in animals infected with RRV during the study period.

DISCUSSION

The present study is the first to comprehensively investigate the adaptation, growth, virulence, and innate immune response for a wild-type and two mutant human RV isolates in a human intestinal cell line and in animals. We took advantage of the availability of a complete passage history of candidate vaccine CDC-9 strain and found that wild-type virus grew poorly in cell cultures and induced predominantly proinflammatory response and mild diarrhea in neonatal rats. In contrast, we found that mutant CDC-9 P44/P45 grew to much higher titers in Caco-2 cells as well as Vero and MA104 cells, induced lower inflammatory responses *in vitro* and *in vivo*, was shed at lower

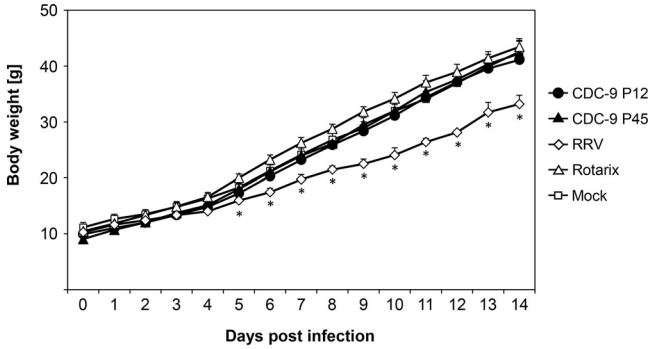

FIG 7 No differences in body weight gain after infection with CDC-9 strains and Rotarix. Five-day-old rat pups were inoculated with 1×10^6 FFU of the respective viruses or clarified Vero cell culture supernatants in IMDM as a mock infection control. Body weights of rats were measured daily. The data are means for 10 (days 0 to 4) and 5 (days 5 to 14) animals, with 3 standard errors. Differences in body weight gain among groups were analyzed using 2-way ANOVA with Bonferroni posttest comparison. There were no differences in body weight gain in animals that received CDC-9 P12, CDC-9 P45, and Rotarix and mock infection controls. RRV-infected animals had significantly lower body weight gain from day 5 to 14 than those in the other 4 groups (*, $P \leq 0.05$).

levels, and induced no diarrhea in neonatal rats. The present study demonstrated that CDC-9 P44/45 was attenuated and safe in animals.

The mechanisms for RV attenuation are not known and may involve sequence changes in one or several gene segments (17, 25). Of the 10 total amino acid sequence changes identified in VP1, VP4, VP6, NSP1, and NSP5 of CDC-9 P44/45, 6 occurred in VP4, including point mutations in fusion domain and a membrane interaction loop in VP5. Of interest, 3 of the 6 changes also occurred at the same locations in VP4 of Rotarix. Since VP4 is involved in membrane penetration and viral entry, infectivity, and virulence, those point mutations could contribute to the enhanced growth of mutant CDC-9 *in vitro* and its reduced shedding in neonatal rats. Our results agree with published reports showing that the VP4 sequence from strains associated with asymptomatic infections differed from those of virulent strains (26) and that the attenuated strain 89-12 shed less than virulent wild-type strain in children (25). However, which genes or what mutations were responsible for the attenuation of strain 89-12 could not be determined, because its wild-type strain was not available for analysis. Of interest, we showed that CDC-9 underwent 1 additional amino acid change in VP4 and a 10-amino-acid deletion in VP2 from P28 to P45 in Vero cells. However, we observed equivalent growth in cells and similar infectivity and host responses of the two mutants in rats, indicating that the deletion in VP2 has no major effect on the structure and function of CDC-9.

In addition to reduced shedding, we showed that CDC-9 P45 did not induce any diarrhea and thus was fully attenuated in neonatal rats, whereas wild-type CDC-9 induced mild diarrhea in some animals. We could document for the first time an association between the adaptation in Vero cells and the associated sequence changes in VP4 of a human RV and its weakened virulence in animals. Our findings agree with published studies on other viruses. Mumps, measles, and foot-and-mouth disease viruses at low passage numbers retained the capacity to induce clinical signs of disease and be shed, whereas higher passages of the viruses failed to do so (27–29). Cell culture-passaged oral polio vaccine had defined mutations in the genome that were in line with low neurovirulence but increased protection against infection with wild-type polio strains (30). Similar findings were reported in the literature for high-passage-number rubella virus strains that grew significantly better *in vitro* but were shed less in monkeys than low-passage-number virus (8, 31). Of note, in contrast to published studies indicating that diarrhea was induced in neonatal rats with RRV infection (2×10^7 to 6.75×10^8 PFU) (32, 33), the lack of diarrhea induction in our study was most likely due to the much lower virus titer used (10^6 FFU). Nevertheless, our study

showed that RRV-infected rats had a significantly reduced gain in body weight, as previously reported (32).

The induction of IFN pathways by RV has been subject of many studies, yet no direct comparison of an attenuated strain versus its original counterpart has been done. We chose to investigate the STAT protein family, with a particular focus on the transcription factor STAT1 which when phosphorylated played a critical role in inducing a host antiviral response after activation of various cytokine receptors (34). On the other hand, viruses have developed counteracting factors to prevent STAT1 phosphorylation and transport into the nucleus (35). For example, RV strains RRV and Wa blocked IFN-induced gene expression, allowing STAT1 and STAT2 phosphorylation but preventing nuclear accumulation to evade the host response (36). Here, we showed that wild-type CDC-9 P11 induced phosphorylation of STAT1 comparable to that induced by RRV, but both mutants, particularly CDC-9 P44, did not activate STAT1 phosphorylation. This dampened STAT1 expression could antagonize host antiviral responses by blocking the expression of genes encoding type I and II interferons and help explain the 2-log-higher growth of mutant CDC-9 than wild-type virus. These findings appear to corroborate the lack of type I IFN expression in infected Caco-2 cells and the significant reduction in levels of type II IFN in sera of CDC-9 P45 infected rats compared to those of wild-type virus-infected animals. Our study clearly showed different STAT1 profiles in response to wild-type and mutant CDC-9 infections in Caco-2 cells; further studies are needed to identify the gene(s) and specific amino acid mutations that contribute to the differences in the induction of innate immune responses.

We observed differential expression of cytokines and chemokines in Caco2 cells and neonatal rats infected with wild-type and attenuated CDC-9. Attenuated CDC-9 induced enhanced expression of immunomodulatory cytokines like IL-6 and reduced expression of proinflammatory cytokines like IL-1β and IFN-γ in both *in vitro* and *in vivo* analyses. These results are more comparable to those from Rotarix infection than those from wild-type CDC-9, corroborating reduction in shedding and lack of diarrhea from CDC-9 P45 infection in neonatal rats. Previous studies also reported increased expression of IL-6, IFN-γ, tumor necrosis factor alpha (TNF-α), and IL-10 in sera of piglets and children with RV infection (37, 38), though it was not clear whether those findings were relevant to RV attenuation and infection. In addition, in a murine model, heterologous infection with simian RRV induced IFN transcripts and inflammatory cytokine response (39).

In conclusion, we showed that mutant CDC-9 with several defined sequence changes in VP4 and a few other genes was able to grow to high titers and induced a more immunomodulatory phenotype than wild-type virus in cell culture. We further demonstrated that mutant CDC-9 was shed less, induced reduced inflammatory response and no disease, and had no impact on body weight gain in neonatal rats; thus, it is considered attenuated and safe. Studies are in progress to define specific mutations and signatures that are responsible for the enhanced growth *in vitro* and attenuation in animals. Our findings support ongoing efforts to test the safety and efficacy of attenuated CDC-9 as a new candidate vaccine for live oral or inactivated parenteral administration.

MATERIALS AND METHODS

Virus preparation and titration. CDC-9 was isolated from a child hospitalized with diarrhea in the United States by 11 initial passages in MA104 cells. The virus was adapted in Vero cells, including 3 rounds of limiting dilution and plaque purification, and further passaged a total of 45 times. CDC-9 at passages 11 and 12 in MA104 cells and passages 28, 44, and 45 in Vero cells was used for different *in vitro* and *in vivo* testing. RRV and Rotarix were cultivated in MA104 cells. Infected cultures were harvested at 4 or 5 dpi by freeze-thawing. Virus in supernatants was clarified by centrifugation at 8,000 rpm for 30 min. Mock inoculum was generated by cultivating Vero cells for 5 days in the same manner.

Titration of cultivated virus strains was performed by an immunospot assay. In brief, MA104 cells were seeded in 96-well plates. After reaching confluence, cells were washed twice with serum-free Iscove's modified Dulbecco medium (IMDM). Serial dilutions of viruses were performed in medium, and cells were infected for 18 h. Cells were fixed and incubated with a rabbit anti-Wa antibody followed by incubation with a peroxidase-labeled goat anti-rabbit IgG antibody. Staining was performed with KPL True Blue peroxidase (VWR, Radnor, PA). Plates were scanned by using a CTL analyzer (Cellular Tech-

nology, Ltd., Beaverton, OR). Stained cells were counted in at least 2 dilutions, and the number of FFU per milliliter was calculated.

Sequencing of virus strains. RNA from RV-infected cell culture was extracted by incubation with TRIzol LS reagent (Life Technologies, Carlsbad, CA) followed by chloroform (Sigma-Aldrich, St. Louis, MO) addition. After centrifugation, the aqueous phase was removed, and ice-cold isopropanol was added. RNA was pelleted, air dried, and resuspended with nuclease-free water. RNA concentration was measured with a NanoDrop instrument (Thermo Fisher, Waltham, MA). Samples were treated with DNase I (Ambion; Thermo Fisher, Waltham MA) according to the manufacturer's instruction. For rRNA removal and library preparation, a human, mouse, and rat rRNA depletion kit and an NEB Ultra II RNA library preparation kit (NEB, Ipswich, MA) were used according to the manufacturer's instructions. Sequencing was performed with an Illumina MiSeq V2 reagent kit (500 cycles; Illumina, San Diego, CA). Data were analyzed with Geneious (version 10.1.3; Biomatters, Newark, NJ) or CLC Genomics Workbench (version 10.0.1; Qiagen, Germantown, MD).

Infection of human intestinal carcinoma cells. Human intestinal carcinoma cells (Caco-2) cells were cultivated in Dulbecco's modified Eagle medium (DMEM; Gibco, Thermo Fisher, Waltham, MA) with neomycin (Gibco, Thermo Fisher), fetal bovine serum (Gibco, Thermo Fisher), and nonessential amino acids (Gibco, Thermo Fisher). For growth curve analysis, cells were seeded in 24-well plates for 5 days and infected with CDC-9 P11, CDC-9 P28, CDC-9 P44, or RRV at a multiplicity of infection (MOI) of 0.1 for 1 h. Infection medium was removed, and fresh DMEM was added to cells. Infected cells and supernatants were harvested every 12 h up to 84 h, and RV titration was performed as described above. For gene analysis and cytokine detection, Caco-2 cells were infected at an MOI of 0.2 with CDC-9 P11, CDC-9 P28, CDC-9 P44, or RRV for 1 h. Infection media were removed, and fresh DMEM was added to the cells. Cells and supernatants were collected separately at 0, 6, and 24 h postinfection and subsequently processed for the respective assays.

Quantification of transcription factor expression. The phosphorylation of the transcription factor STAT1 was analyzed by using the phosphor-STAT1 (pSer^{727}) and pan-STAT1 enzyme-linked immunosorbent assay (ELISA) kit (Sigma-Aldrich, St. Louis, MO) according to the manufacturer's instructions. In brief, cells were harvested at various time points postinfection and treated with the supplied cell lysis buffer. For measurement of human p-STAT1 (Ser^{727}) and pan-STAT1, the left side of the 96-well plate was coated with anti-p-STAT1 (Ser^{727}) antibody and the right side was coated with an anti-pan-STAT1 antibody. Serially diluted cell lysates and controls were added to the 96-well plate, and phosphorylated STAT1 and pan-STAT1 present in the sample bound to the immobilized respective antibodies on the plate. After washing of the wells, biotinylated anti-STAT1 was used to detect p-STAT1 (Ser^{727}) or pan-STAT1. Detection was carried out by adding horseradish peroxidase (HRP)-conjugated streptavidin-TMB (3,3′,5,5′-tetramethylbenzidine) for 30 min for color development, and the reaction was stopped with the supplied stop solution. Optical density was determined with an enzyme immunoassay (EIA) reader at 450 nm. Mean absorbance was calculated for each sample. For Western blot analysis, cells were harvested at various time points postinfection and treated with radioimmunoprecipitation assay (RIPA) buffer supplemented with protease and phosphatase inhibitors (Thermo Scientific, Waltham, MA) for 30 min on ice. Lysates were supplemented with equal amounts of 2× sodium dodecyl sulfate-polyacrylamide gel electrophoresis (SDS-PAGE) loading dye containing 10% β-mercaptoethanol, denatured at 97°C for 5 min, and separated on 10% SDS-PAGE gels. Proteins were transferred to nitrocellulose membranes (Bio-Rad, Hercules, CA) and detected with the following antibodies: p-STAT1 (Tyr701) (clone 7649), p-STAT2 (Tyr690) (clone 4441), p-STAT3 (Tyr705) (clone 9145), p-STAT5 (Tyr694) (clone 4322), p-STAT6 (Tyr641) (clone 9361), β-actin (clone 4967), and HRP-linked anti-rabbit IgG (secondary antibody) (all from Cell Signaling Technology, Danvers, MA) according to the manufacturer's instructions. Blots were developed with an Amersham ECL Prime Western blot detection reagent (GE Healthcare, Pittsburgh, PA) and exposed to an autoradiography film (GE Healthcare, Pittsburgh, PA).

Cytokine and chemokine quantification. The expression of cytokines and chemokines in the supernatants of Caco-2 cells after infection with different viruses was assessed by using flow cytometry-based kits, including the LEGENDplex human Th cytokine panel (BioLegend, San Diego, CA), the CBA human inflammatory cytokine kit, and the CBA human chemokine kit (BD, San Jose, CA), according to the respective manufacturer's instructions. Cytokine and chemokine expression in sera of neonatal rats was analyzed by using a LEGENDplex rat inflammation panel and a LEGENDplex Th cytokine panel (BioLegend, San Diego, CA) according to the manufacturer's instructions. Data were analyzed with BD FACS DIVA software, GraphPad Prism version 5 (San Diego, CA), and LEGENDplex version 8 (BioLegend, San Diego, CA).

Infection of neonatal rats. Timed pregnant female Lewis rats (LEW/SsNHsd) were obtained from Envigo (East Millstone, NJ). One day after birth, pups were randomly distributed to a litter size of 10 pups per mother to ensure comparable nutrition availability. Five-day-old pups were infected by oral gavage with 1×10^6 FFU of CDC-9 P12, CDC-9 P45, RRV, or Rotarix or given a mock infection control diluted in IMDM. Body weight was checked, and diarrhea was scored daily according to the diarrhea index (Table 2), where a score of >2 was considered diarrhea. Animals in different groups were coded and monitored daily for up to 14 days in an unbiased manner. On day 4 and day 14 postinfection, 5 animals in each group were euthanized, and whole blood was collected for serum preparation. Rectal swabs were collected daily from infected neonatal rats up to 14 dpi and placed in 0.5 ml Rotaclone diluent. Analysis of shedding was performed with Premier Rotaclone EIA (Meridian, Cincinnati, OH) according to the manufacturer's instructions.

TABLE 2 Diarrhea index

Score	Description
0	Normal feces
1	Unusually loose, yellow stool
2	Mucus with liquid stool, some loose but still solid
3	Totally loose yellow-green stool
4	Large amount of watery feces

All experiments involving animals were approved by the International Animal Care and Use Committee (IACUC) of the CDC and conducted in accordance with the ethical guidelines for animal experiments and safety guidelines.

Statistical analysis. Graphs were generated by Microsoft Excel or GraphPad Prism 5.02. Statistical analysis was performed by using GraphPad Prism 5.02. 2-way analysis of variance (ANOVA) with Bonferroni posttest comparison of replicate means to determine statistical significance of RV shedding and body weight gain in neonatal rats. For all other analysis, we assumed no normal distribution of data and used the Mann-Whitney test (two-tailed). *P* values equal to or lower than 0.05 were considered statistically significant.

ACKNOWLEDGMENTS

This study was supported in part by the Centers for Disease Control and Prevention, Atlanta, GA, USA.

The findings and conclusions in this report are those of the authors and do not necessarily represent the official position of the Centers for Disease Control and Prevention.

Yuhuan Wang and Baoming Jiang hold patents through CDC for RV vaccine strain CDC-9. We have no other conflicts of interest.

REFERENCES

1. Sabin AB, Hennessen WA, Winsser J. 1954. Studies on variants of poliomyelitis virus. I. Experimental segregation and properties of avirulent variants of three immunologic types. J Exp Med 99:551–576. https://doi.org/10.1084/jem.99.6.551.
2. Katz SL, Kempe CH, Black FL, Lepow ML, Krugman S, Haggerty RJ, Enders JF. 1960. Studies on an attenuated measles-virus vaccine. VIII. General summary and evaluation of the results of vaccination. Am J Dis Child 100:942–946. https://doi.org/10.1001/archpedi.1960.04020040944023.
3. Hilleman MR, Buynak EB, Weibel RE, Stokes J, Jr. 1968. Live, attenuated mumps-virus vaccine. N Engl J Med 278:227–232. https://doi.org/10.1056/NEJM196802012780501.
4. Plotkin SA, Farquhar JD, Katz M, Buser F. 1969. Attenuation of RA 27-3 rubella virus in WI-38 human diploid cells. Am J Dis Child 118:178–185. https://doi.org/10.1001/archpedi.1969.02100040180004.
5. Takahashi M, Okuno Y, Otsuka T, Osame J, Takamizawa A. 1975. Development of a live attenuated varicella vaccine. Biken J 18:25–33.
6. Barrett PN, Mundt W, Kistner O, Howard MK. 2009. Vero cell platform in vaccine production: moving towards cell culture-based viral vaccines. Expert Rev Vaccines 8:607–618. https://doi.org/10.1586/erv.09.19.
7. Plotkin S. 2014. History of vaccination. Proc Natl Acad Sci U S A 111:12283–12287. https://doi.org/10.1073/pnas.1400472111.
8. Parkman PD, Meyer HM, Jr, Kirschstein RL, Hopps HE. 1966. Attenuated rubella virus. I. Development and laboratory characterization. N Engl J Med 275:569–574. https://doi.org/10.1056/NEJM196609152751101.
9. Dang DA, Nguyen VT, Vu DT, Nguyen TH, Nguyen DM, Yuhuan W, Baoming J, Nguyen DH, Le TL, Rotavin M. 2012. A dose-escalation safety and immunogenicity study of a new live attenuated human rotavirus vaccine (Rotavin-M1) in Vietnamese children. Vaccine 30(Suppl 1):A114–A121.
10. Bhandari N, Rongsen-Chandola T, Bavdekar A, John J, Antony K, Taneja S, Goyal N, Kawade A, Kang G, Rathore SS, Juvekar S, Muliyil J, Arya A, Shaikh H, Abraham V, Vrati S, Proschan M, Kohberger R, Thiry G, Glass R, Greenberg HB, Curlin G, Mohan K, Harshavardhan GV, Prasad S, Rao TS, Boslego J, Bhan MK, India Rotavirus Vaccine Group. 2014. Efficacy of a monovalent human-bovine (116E) rotavirus vaccine in Indian infants: a randomised, double-blind, placebo-controlled trial. Lancet 383:2136–2143. https://doi.org/10.1016/S0140-6736(13)62630-6.
11. Ward RL, Bernstein DI. 2009. Rotarix: a rotavirus vaccine for the world. Clin Infect Dis 48:222–228. https://doi.org/10.1086/595702.
12. Bernstein DI, Smith VE, Sherwood JR, Schiff GM, Sander DS, DeFeudis D, Spriggs DR, Ward RL. 1998. Safety and immunogenicity of live, attenuated human rotavirus vaccine 89–12. Vaccine 16:381–387. https://doi.org/10.1016/s0264-410x(97)00210-7.
13. Mattion NM, Mitchell DB, Both GW, Estes MK. 1991. Expression of rotavirus proteins encoded by alternative open reading frames of genome segment 11. Virology 181:295–304. https://doi.org/10.1016/0042-6822(91)90495-w.
14. Feng N, Sen A, Wolf M, Vo P, Hoshino Y, Greenberg HB. 2011. Roles of VP4 and NSP1 in determining the distinctive replication capacities of simian rotavirus RRV and bovine rotavirus UK in the mouse biliary tract. J Virol 85:2686–2694. https://doi.org/10.1128/JVI.02408-10.
15. Feng N, Yasukawa LL, Sen A, Greenberg HB. 2013. Permissive replication of homologous murine rotavirus in the mouse intestine is primarily regulated by VP4 and NSP1. J Virol 87:8307–8316. https://doi.org/10.1128/JVI.00619-13.
16. Broome RL, Vo PT, Ward RL, Clark HF, Greenberg HB. 1993. Murine rotavirus genes encoding outer capsid proteins VP4 and VP7 are not major determinants of host range restriction and virulence. J Virol 67:2448–2455. https://doi.org/10.1128/JVI.67.5.2448-2455.1993.
17. Hoshino Y, Saif LJ, Kang SY, Sereno MM, Chen WK, Kapikian AZ. 1995. Identification of group A rotavirus genes associated with virulence of a porcine rotavirus and host range restriction of a human rotavirus in the gnotobiotic piglet model. Virology 209:274–280. https://doi.org/10.1006/viro.1995.1255.
18. Azim T, Ahmad SM, Sefat EK, Sarker MS, Unicomb LE, De S, Hamadani JD, Salam MA, Wahed MA, Albert MJ. 1999. Immune response of children who develop persistent diarrhea following rotavirus infection. Clin Diagn Lab Immunol 6:690–695. https://doi.org/10.1128/CDLI.6.5.690-695.1999.
19. Wang Y, Dennehy PH, Keyserling HL, Tang K, Gentsch JR, Glass RI, Jiang B. 2007. Rotavirus infection alters peripheral T-cell homeostasis in children with acute diarrhea. J Virol 81:3904–3912. https://doi.org/10.1128/JVI.01887-06.
20. Barro M, Patton JT. 2007. Rotavirus NSP1 inhibits expression of type I interferon by antagonizing the function of interferon regulatory factors

IRF3, IRF5, and IRF7. J Virol 81:4473–4481. https://doi.org/10.1128/JVI.02498-06.
21. Barro M, Patton JT. 2005. Rotavirus nonstructural protein 1 subverts innate immune response by inducing degradation of IFN regulatory factor 3. Proc Natl Acad Sci U S A 102:4114–4119. https://doi.org/10.1073/pnas.0408376102.
22. Sen A, Rott L, Phan N, Mukherjee G, Greenberg HB. 2014. Rotavirus NSP1 protein inhibits interferon-mediated STAT1 activation. J Virol 88:41–53. https://doi.org/10.1128/JVI.01501-13.
23. Holloway G, Dang VT, Jans DA, Coulson BS. 2014. Rotavirus inhibits IFN-induced STAT nuclear translocation by a mechanism that acts after STAT binding to importin-alpha. J Gen Virol 95:1723–1733. https://doi.org/10.1099/vir.0.064063-0.
24. Esona MD, Foytich K, Wang Y, Shin G, Wei G, Gentsch JR, Glass RI, Jiang B. 2010. Molecular characterization of human rotavirus vaccine strain CDC-9 during sequential passages in Vero cells. Hum Vaccin 6:10409.
25. Ward RL, Mason BB, Bernstein DI, Sander DS, Smith VE, Zandle GA, Rappaport RS. 1997. Attenuation of a human rotavirus vaccine candidate did not correlate with mutations in the NSP4 protein gene. J Virol 71:6267–6270. https://doi.org/10.1128/JVI.71.8.6267-6270.1997.
26. Flores J, Midthun K, Hoshino Y, Green K, Gorziglia M, Kapikian AZ, Chanock RM. 1986. Conservation of the fourth gene among rotaviruses recovered from asymptomatic newborn infants and its possible role in attenuation. J Virol 60:972–979. https://doi.org/10.1128/JVI.60.3.972-979.1986.
27. Buynak EB, Hilleman MR. 1966. Live attenuated mumps virus vaccine. 1. Vaccine development. Proc Soc Exp Biol Med 123:768–775. https://doi.org/10.3181/00379727-123-31599.
28. Enders JF, Katz SL, Milovanovic MV, Holloway A. 1960. Studies on an attenuated measles-virus vaccine. I. Development and preparations of the vaccine: technics for assay of effects of vaccination. N Engl J Med 263:153–159. https://doi.org/10.1056/NEJM196007282630401.
29. Sa-Carvalho D, Rieder E, Baxt B, Rodarte R, Tanuri A, Mason PW. 1997. Tissue culture adaptation of foot-and-mouth disease virus selects viruses that bind to heparin and are attenuated in cattle. J Virol 71:5115–5123. https://doi.org/10.1128/JVI.71.7.5115-5123.1997.
30. Pliaka V, Kyriakopoulou Z, Markoulatos P. 2012. Risks associated with the use of live-attenuated vaccine poliovirus strains and the strategies for control and eradication of paralytic poliomyelitis. Expert Rev Vaccines 11:609–628. https://doi.org/10.1586/erv.12.28.
31. Meyer HM, Jr, Parkman PD, Panos TC. 1966. Attenuated rubella virus. II. Production of an experimental live-virus vaccine and clinical trial. N Engl J Med 275:575–580. https://doi.org/10.1056/NEJM196609152751102.
32. Ciarlet M, Conner ME, Finegold MJ, Estes MK. 2002. Group A rotavirus infection and age-dependent diarrheal disease in rats: a new animal model to study the pathophysiology of rotavirus infection. J Virol 76:41–57. https://doi.org/10.1128/jvi.76.1.41-57.2002.
33. Crawford SE, Patel DG, Cheng E, Berkova Z, Hyser JM, Ciarlet M, Finegold MJ, Conner ME, Estes MK. 2006. Rotavirus viremia and extraintestinal viral infection in the neonatal rat model. J Virol 80:4820–4832. https://doi.org/10.1128/JVI.80.10.4820-4832.2006.
34. Platanias LC. 2005. Mechanisms of type-I- and type-II-interferon-mediated signalling. Nat Rev Immunol 5:375–386. https://doi.org/10.1038/nri1604.
35. Nan Y, Wu C, Zhang YJ. 2017. Interplay between Janus kinase/signal transducer and activator of transcription signaling activated by type I interferons and viral antagonism. Front Immunol 8:1758. https://doi.org/10.3389/fimmu.2017.01758.
36. Holloway G, Truong TT, Coulson BS. 2009. Rotavirus antagonizes cellular antiviral responses by inhibiting the nuclear accumulation of STAT1, STAT2, and NF-kappaB. J Virol 83:4942–4951. https://doi.org/10.1128/JVI.01450-08.
37. Azevedo MS, Yuan L, Jeong KI, Gonzalez A, Nguyen TV, Pouly S, Gochnauer M, Zhang W, Azevedo A, Saif LJ. 2005. Viremia and nasal and rectal shedding of rotavirus in gnotobiotic pigs inoculated with Wa human rotavirus. J Virol 79:5428–5436. https://doi.org/10.1128/JVI.79.9.5428-5436.2005.
38. Jiang B, Snipes-Magaldi L, Dennehy P, Keyserling H, Holman RC, Bresee J, Gentsch J, Glass RI. 2003. Cytokines as mediators for or effectors against rotavirus disease in children. Clin Vaccine Immunol 10:995–1001. https://doi.org/10.1128/CDLI.10.6.995-1001.2003.
39. Sen A, Namsa ND, Feng N, Greenberg HB. 2020. Rotavirus reprograms multiple interferon receptors and restricts their intestinal antiviral and inflammatory functions. J Virol 94:e01775-19. https://doi.org/10.1128/JVI.01775-19.